Journal of Alloys and Compounds 509 (2011) 1809–1814

Contents lists available at ScienceDirect

Journal of Alloys and Compounds

journal homepage: www.elsevier.com/locate/jallcom

Structure of a W-enriched phase in Fe–Co–Cr–W–Ga alloys

G.V. Ivanova, N.N. Shchegoleva, V.V. Serikov, N.M. Kleinerman*, E.V. Belozerov

Institute of Metal Physics UB RAS, 18 S. Kovalevskoi Str., 620990 Ekaterinburg, Russia

ARTICLE INFO

Article history:
Received 8 July 2010
Received in revised form 8 October 2010
Accepted 10 October 2010
Available online 21 October 2010

Keywords:
Metals and alloys
Precipitation
Mechanical properties
X ray diffraction
Transmission electron microscopy
Mossbauer spectroscopy

ABSTRACT

Structure of a metastable W-enriched nanophase that is formed in Fe–Co–Cr–W–Ga alloys has been studied using X ray, electron microscopy, and Mossbauer spectroscopy methods. The phase is established to possess a body-centered-tetragonal crystal lattice with the lattice parameters a ≈ 2.96 Å, c ≈ 3.17 Å. The orientational relationships between its lattice and that of the matrix α-Fe based solid solution are determined. It is shown that the phase contains iron, tungsten, and plausibly chromium, being quite inhomogeneous in composition. Moreover, it is likely to be of a variable composition. At room temperature the phase is paramagnetic.

1. Introduction

Magnetically hard alloys on the basis of the Fe–Co–Cr system alloyed with tungsten and gallium possess high strength and a plasticity margin required to prevent brittle fracture of the material when used as a rotor for high speed engines working with speeds higher than 100–150 thousand revolutions per minute. In our previous work [1] structure transformations were studied that take place at different stages of the treatment resulting in a high-coercivity state of the alloys. It was established that in the course of annealings at 640–600 °C in the alloys there takes place a decomposition of the high-temperature α-Fe based solid solution with the formation of a strong magnetic (Fe–Co enriched), weak magnetic (Fe–Cr enriched) phases and disperse W enriched phase.

A preliminary investigation with the help of the Mossbauer method showed [1] that in the Mossbauer spectra of the alloys containing W one can pick out three contributions related to the high-field distribution, one contribution from the low-field distribution, and a paramagnetic contribution. Since no traces of γ-Fe phase were detected in the X ray patterns, an assumption was made that the paramagnetic contribution can be ascribed to the W-enriched phase. The isomeric shift of this spectral component was established to be −0.24 mm/s, which is characteristic of a configuration of the Fe atom neighborhood with the nearest tungsten atoms [2,3]. It is shown that in the samples studied after cold deformation followed by the low-temperature aging this phase contains about 4% Fe charged in the alloys. Supposing that tungsten is localized entirely in this phase and cobalt and chromium are not contained at all, its composition was estimated as Fe_2W_3.

The disperse particles of this phase are suggested to take quite a significant part in the formation of the alloy properties. First [1], they may serve as obstacles for the dislocation motion and favor strengthening of the alloys, increasing stresses, and, consequently, growing contribution of elastic energy in the high-coercivity state. Second, small precipitates of the paramagnetic phase can hinder motion of magnetic domain walls, thus providing a coercivity of 125–190 Oe.

The crystal structure of this phase has not been identified yet. In the X ray diffraction patterns there were observed four weak reflections which were difficult to unambiguously define. In our previous work the phase was supposed to have a body-centered tetragonal (bct) lattice with the parameters a = 5.35 Å and c = 4.28 Å. However, no information on the existence of a compound with such lattice in the alloys containing W, Fe(Cr, Co) is available. As it follows from the phase diagrams, in the systems Fe–W [4, p. 1791] and Co–W [4, p. 1257] there exist the following phases: Fe_2W with a hexagonal lattice of the $MgZn_2$ type, δ-FeW with a rhombic lattice of the MoNi type, Fe_7W_6 and Co_7W_6 with a rhombohedral, and Co_3W with a hexagonal structure of the Ni_3Sn type. In the alloys Fe–W–Cr and W–Cr–Co [5] there exists the σ phase with a tetragonal lattice. It is reported in [6] that in the course of a discontinuous decomposition of an initial solid solution in the alloys Fe–Mo and Fe–W there takes place precipitation of a metastable η′ phase which in the alloys Fe–Mo possesses a body-centered-rhombic lattice with the parameters a = 2.91 Å, *b* = 2.97 Å, *c* = 3.22 Å.

* Corresponding author. Tel.: +7 343 378 37 24; fax: +7 343 374 52 44.
E-mail address: kleinerman@imp.uran.ru (N.M. Kleinerman).

0925-8388/$ – see front matter © 2010 Elsevier B.V. All rights reserved.
doi:10.1016/j.jallcom.2010.10.046

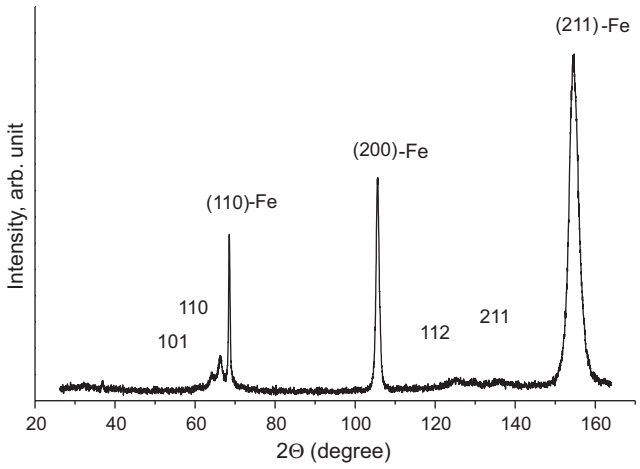

Fig. 1. X ray diffraction pattern for the alloy Fe–22Cr–15Co–9W–3Ga after quenching from 1150 °C, cold rolling, and low-temperature annealing. In brackets indices of the α phase reflections are shown; arrows point to the reflections from the W enriched phase.

The work presented deals with a detailed study of the structure of a W-enriched disperse phase in the alloys Fe–Cr–Co–W–Ga.

2. Experimental

Alloys of the compositions Fe–22Cr–15Co–(8–10)W–(0–4)Ga were melted in an induction furnace in argon atmosphere from the charged materials of purity no less than 99.95. After homogenization at 1200 °C for 2 h the ingots were hot-forged at 1100–1500 °C. After the then hot-rolled sheets were quenched from 1150 °C for solid solution state, the alloys were subjected to cold rolling with a reduction of up to 70%. The heat treatment for a high-coercivity state consisted in annealing at 620–640 °C for 20–45 min followed by annealing at 600 °C for 30–60 min. For comparison, samples which did not experience cold rolling were heat-treated as well.

The phase composition of the samples was controlled with the help of X-ray analysis. The electron-microscopy and electron diffraction studies were performed using a microscope JEM-200CX. The foils were prepared by electrolytically polishing in a mixture of chromium trioxide and orthophosphoric acid. Mossbauer spectra were taken at 300 K in the constant acceleration mode with a source Co^{57} in the chromium matrix. Measurements were carried out on foils with dimensions of 10 mm × 10 mm × 0.03 mm by means of an MC1101 spectrometer (512 channels, 5–8 × 10^5 count·channel, and the quality ratio of the spectra 70–80). The spectra were processed with allowance for the effects of self-absorption using the MS TOOLS program package, which makes it possible both to directly fit the spectra with a number of subspectra and to construct multi-core distributions of the probability density of hyperfine parameters on a reasonable assumption that different structural constituents exhibit different correlation dependences for, at least, two Mossbauer parameters [7]. The isomeric shifts of spectral components were determined with respect to the spectrum of α-Fe.

3. Results and discussion

3.1. X ray analysis

Fig. 1 shows an X ray diffraction pattern for the alloy Fe–22Cr–15Co–9W–3Ga after quenching from 1150 °C, cold rolling, and subsequent aging by the regime 640° 40 min + 600° 1 h. One can see the reflections of the α-Fe based solid solution and additional very weak reflections which belong to the W-enriched phase under study. If to indicate these reflections as is shown in Fig. 1, the observed phase turns out to have a bct lattice with the parameters a = 2.96 Å, c = 3.17 Å, which is similar to the η′-phase discovered by the authors of [6]. In the diffraction pattern reflections (2 0 0) and (0 0 2) of this phase, which are not forbidden by the extinction rules, are lacking, evidently, because of their weakness. Although the phase detected in our studies has a tetragonal lattice rather than a rhombohedral one as in [6], we would call it in what follows an η′ phase.

From the positions of the (1 1 0) and (1 0 1) reflections in the X ray diffraction pattern the parameters of the tetragonal lattice of this phase were determined for the alloys of different compositions. Since these reflections, even when taken in the softest Cr radiation, are located in small angles, the accuracy of such measurements is certainly low: $\Delta a \pm 0.01$ Å, $\Delta c \pm 0.02$ Å. However, the lattice parameters for the alloys of different compositions vary in the range from a = 2.94 Å, c = 3.15 Å to a = 2.97 Å, c = 3.18 Å, which means that the scatter at least in a exceeds the error. This is evidently related to the fact that the η′ phase has different concentrations of W in different alloys and, consequently, it can be of a variable composition.

It is interesting to note that in the X ray patterns that were taken from the samples aged immediately after quenching from 1150 °C the reflections of this phase were virtually absent. Plausibly, the reason for this consists in a higher rate of diffusion in the deformed samples and, correspondingly, faster process of formation of the W enriched phase.

3.2. Electron microscopy examination

In Fig. 2a and b a bright-field micrograph and electron diffraction pattern are shown for the sample Fe–22Cr–15Co–9W–0.5Ga after cold rolling and subsequent aging. A part of reflections are interpreted as reflections from a single-crystal region of the α phase, with the indices shown to the right of each of them. The other reflections belong to the W enriched phase. All of them can easily be indicated as reflections of a phase with the tetragonal lattice with the parameters a = 2.96 Å, c = 3.17 Å, all the indices being shown to the right of each reflection. Interestingly, the same reflections {1 0 1, 1 1 0, 2 1 1, 1 1 2} were revealed in the electron diffraction patterns for many other specimens, unlike the reflections {2 0 0} and (0 0 2). The dark-field micrograph taken in reflection {1 0 1} of the η′ phase is shown in Fig. 2c. The phase is seen to be disperse, (40–70) nm in size; in Fig. 2a its particles look black. The completely analogous results were gained for the alloys with different Ga contents.

Fig. 3 presents the electron micrograph for the sample Fe–21Cr–15Co–9W–0.5Ga annealed immediately after quenching from 1150 °C; in the insert the electron diffraction pattern is shown (the zone axis is {1 0 0}-α). The black spots are the η′ phase regions. It is clearly seen that with such orientation of the foil there are present both rounded and plate-shaped regions of this phase. A close look opens up that the plates are composed of lens-shaped regions 20 nm thick constituting a chain. The "lens" plane is parallel to the crystallographic plane {1 1 0}-α. Unfortunately, the tested samples of the alloys subjected to cold rolling prior to the low-temperature annealing represented a texture: planes {1 1 2}-α were parallel to the surface of the platelike samples. Feasibly, this accounts for the fact that in the corresponding micrographs the η′ phase particles were as a rule rounded (see Fig. 2a).

The volume fraction of the η′ phase was estimated from the electron micrographs to be (7–9)% the whole sample volume, taking into account the above observation of the particles in the form of lens 20 nm thick.

An additional holding of the annealed samples at 750 °C for 5 min or at 640 °C for 40 min resulted in the appearance in the electron diffraction patterns, along with the reflections from the α and η′ phases, some extra weak reflections. This fact enables us to suppose that the η′ phase started transforming into the equilibrium phase just as in [6]. Obviously, the η′ phase in the alloys under study is also metastable.

3.3. Orientational relationships between the lattices of phases

Based on many electron diffraction patterns, the following orientational relationships between the crystal lattices of two phases were for certain established: $(\bar{1}\,\bar{1}\,1)$-α || $(1\,\bar{1}\,0)$-η′, $(\bar{3}\,1\,1)$-α || $(0\,\bar{1}\,1)$-

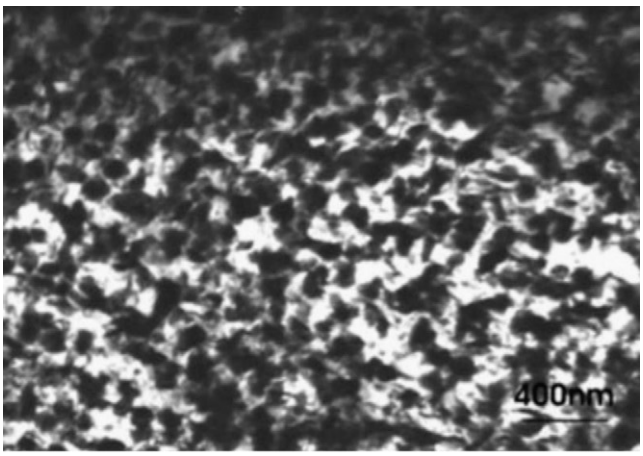

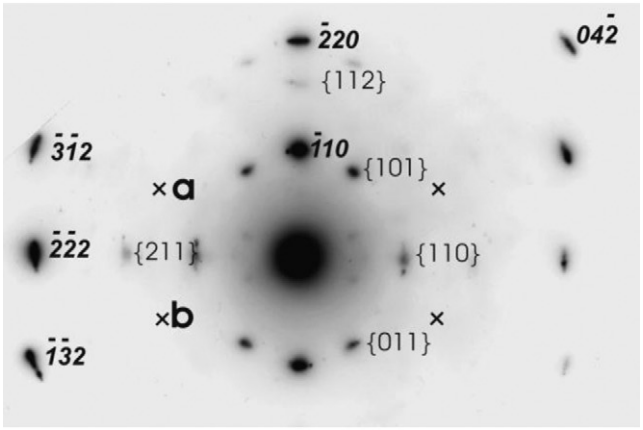

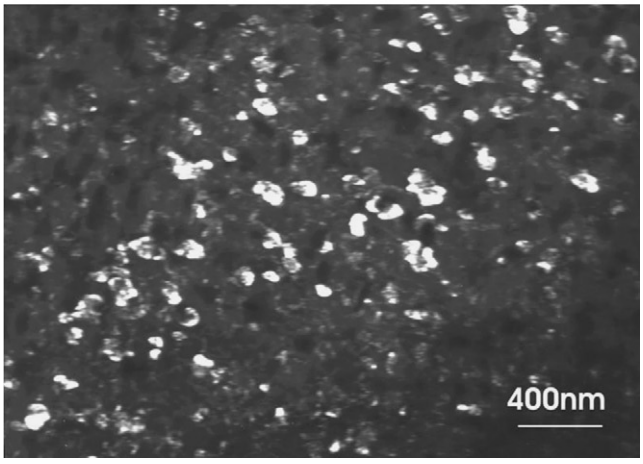

Fig. 2. Electron microscopy micrographs of the structure (a – bright-field, b – dark-field in reflection {1 0 1}) and electron diffraction pattern (c) for the alloy Fe–22Cr–15Co–9W–0.5Ga treated for optimal properties. In the electron diffraction pattern indices of reflections are shown on the right. The zone axis is [1 1 2]-α. Indices are: bold italic for α phase, straight weaker in braces for η′ phase. Besides there are seen also extra reflections resulting from the double reflection effect.

η′, and $(1\,\bar{3}\,1)$-α || $(1\,0\,\bar{1})$-η′, with the directions [1 1 2]-α || [1 1 1]-η′ lying in these planes. It can easily be ascertained that there can exist 24 possible orientations of the η′-phase lattice relative to that of the α phase.

In Fig. 4 a stereographic projection of a crystal of the α phase in the orientation corresponding to that in Fig. 2b is shown (recall that the reflection poles which are present in the electron diffraction pattern are located on the outer circle of the stereographic projection). Localization of some poles of 6 possible orientations of the η′

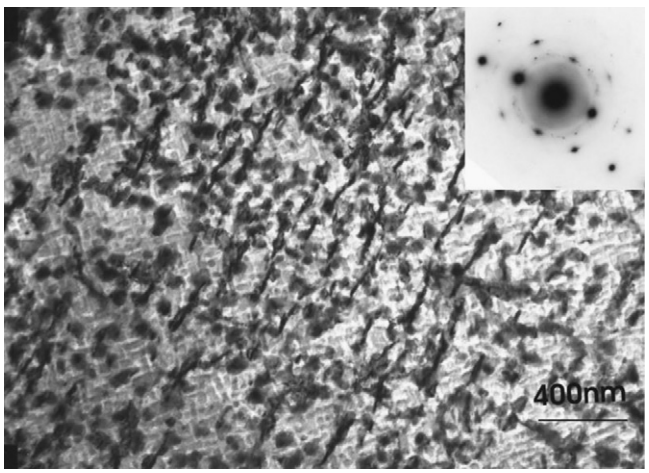

Fig. 3. Electron micrograph of the microstructure for the sample Fe–22Cr–15Co–9W–0.5Ga subjected to the low-temperature annealings immediately after quenching from 1150 °C. In the insert, the diffraction pattern with the zone axis ⟨100⟩-α is shown.

phase is indicated in the projection as example. The poles of different orientations are marked by different symbols. It is seen that a part of the poles of different orientations are virtually superimposed. In particular, poles {1 0 1} of three different orientations of the η′ phase coincide with each other and pole $(\bar{3}\,1\,1)$-α; the three other {1 0 1}-η′, with $(1\,\bar{3}\,1)$-α; poles {1 1 0}-η′ coincide in two with $(\bar{1}\,\bar{1}\,1)$ and 1 1 1)-α; four poles {1 1 2}-η′ are superimposed onto $(\bar{1}\,1\,0)$-α, etc. A consideration of all possible orientations of the η′ phase results in a conclusion that each pole {1 1 1}-α coincides with 6 poles (1 1 0)-η′ and 6 poles {2 1 1}-η′; each pole {1 1 0}-α, with 4 poles (1 1 2)-η′; each {3 1 1}-α, with 4 poles {1 0 1}-η′. At the same time, no poles (0 0 1) and {1 0 0}-η′ of different orientations are superimposed at all.

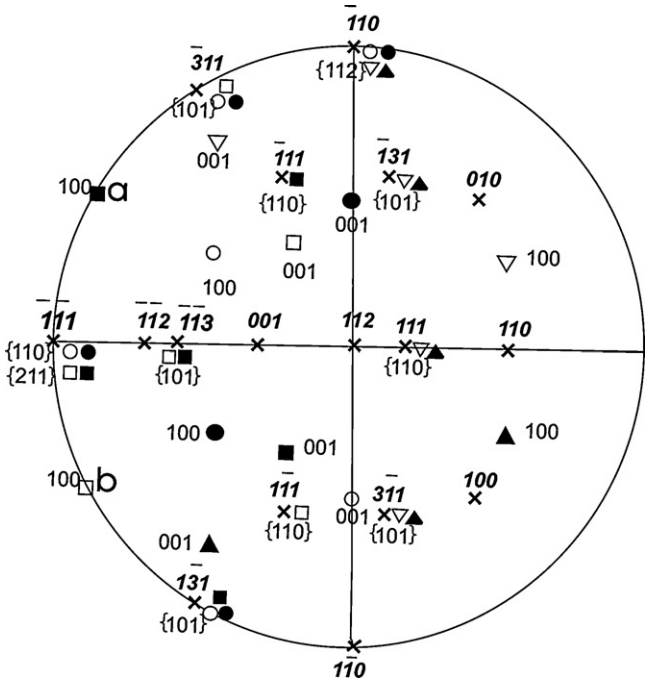

Fig. 4. Stereographic projection of the crystal. **x** are poles of the α phase (indices are shown in bold italic). All other symbols are poles of the η′ phase of different orientations (indices are shown in weak straight). Indices of the coinciding poles of different orientations of the η′ phase are taken in braces.

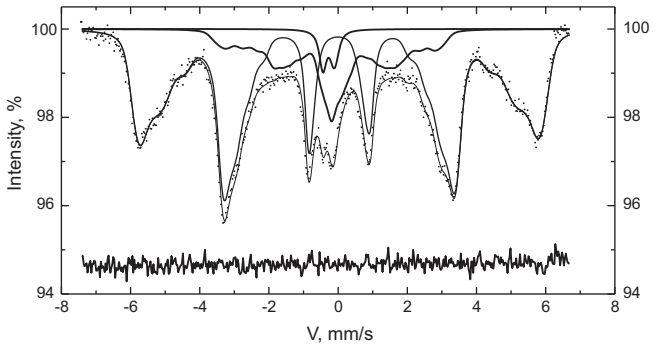

Fig. 5. Mossbauer spectrum for the sample Fe–22Cr–15Co–9W annealed after quenching from 1150 °C and cold rolling.

If to compare the electron diffraction pattern in Fig. 2b with the stereographic projection, one can see that four reflections ({1 0 1}, {1 1 0}, {0 1 1}, and {1 1 2}) in the electron pattern belong to two orientations in the stereographic projection denoted by black and blank circles, whereas {2 1 1}, does not. However, it, together with {1 0 1} and {0 1 1}, belongs to two other orientations denoted as black and blank squares, which do not contribute to ({1 1 0} and {1 1 2}. Evidently, the orientations displayed in the stereographic projection are realized in the sample. The comparison of the structure micrographs in Fig. 2a and b shows that not all regions of the η′ phase shine in its reflection {1 0 1}, which means that in the sample there are regions with the orientations that do not manifest themselves in the stereographic projection.

In full agreement with the above, reflections {1 0 1} and (1 1 0)-η′ in Fig. 2b are strong, whereas {2 1 1} and {1 1 2}, of moderate intensity. It follows from the stereographic projection that one of the poles {2 0 0}-η′ must be located in points **a** and **b**. However, in the electron diffraction pattern in Fig. 2b such reflections are absent. The reason for this is apparently that these reflections are single and therefore very weak. Thus, the above experimental electron diffraction pattern (as well as many other) and the stereographic projection are in a good agreement with the suggested crystal lattice of the η′ phase and its orientational relationships with the matrix.

3.4. Mossbauer study

Additional information on this phase was gained with the help of the Mossbauer method. In Fig. 5 the Mossbauer spectrum for the sample Fe–22Cr–15Co–9W annealed after quenching from 1150 °C and cold rolling is shown together with the contributions from three-core distributions of the density of probabilities $P(H)$ and $P(Q)$ presented in Fig. 6 (here H is the hyperfine field; Q is the quadrupole splitting). The similar spectra were taken and processed for the samples of the alloys containing Ga. One can pick out three regions, of which one corresponds to high hyperfine fields (strong magnetic regions α_1 depleted of chromium), second, to low fields (weak magnetic α_2 regions enriched in chromium), and a paramagnetic doublet shifted relative to the zero point because of an isomeric shift. The quadrupole splitting is known to indicate that the corresponding phase has a crystal lattice with a lowered, with respect to the cubic, symmetry. Hence, the paramagnetic doublet is likely to belong to the η′ phase possessing a tetragonal lattice.

The low-field part of the distribution $P(H)$ in Fig. 6 contains a peak in fields close to zero, which is separated from the rest part of the low-field distribution. It was taken as an indication to construct a four-core distribution $P(H)$, which is shown in Fig. 7 for the alloy Fe–22Cr–15Co–9W. Along with the already described three regions, the forth one was picked out as a poorly resolved sextet in small fields, looking as a singlet. Such a singlet corresponds to a ferromagnetic "phase" with the Curie point slightly higher than room temperature. In what follows we would call this poorly resolved sextet singlet, for simplicity.

The four-core distribution allows one to trace properties of all four "phases". In Fig. 8 linear correlations are shown between the isomeric shift and hyperfine field for all ferromagnetic components and isomeric shift and quadrupole splitting for the paramagnetic doublet and singlet. All the correlation lines in the figure represent different slopes, which supports the validity of the four-core distribution. While discussing these results, one should keep in mind that the presence of an impurity atom in the neighborhood of iron atom affects both the hyperfine field and isomeric shift magnitudes. Thus, Cr decreases hyperfine field and produces a negative isomeric shift up to −0.11 mm/s [8], Co increases the field and makes isomeric shift positive [8], and W significantly diminishes field and produces large negative isomeric shift [2]. As is seen from Fig. 8 the line corresponding to the strong magnetic phase α_1 goes in large fields in the range of close to zero isomeric shifts, which agrees well with the suggestion that the phase contains Fe, Co, and in a small amount Cr. The line of the weak magnetic phase α_2 takes up the range of lower fields with negative isomeric shifts, which means that the phase contains a significant amount of Cr and, apparently, some amount of W. The singlet is situated in extremely low fields and its isomeric shift changes from a small positive to large negative, with the virtually zero quadrupole splitting, see Fig. 7. This "phase" is remarkably enriched in chromium and appears to contain some amount of Co and W in a cubic lattice. Finally, the paramagnetic doublet represents in Fig. 8 a large range of quadrupole splitting

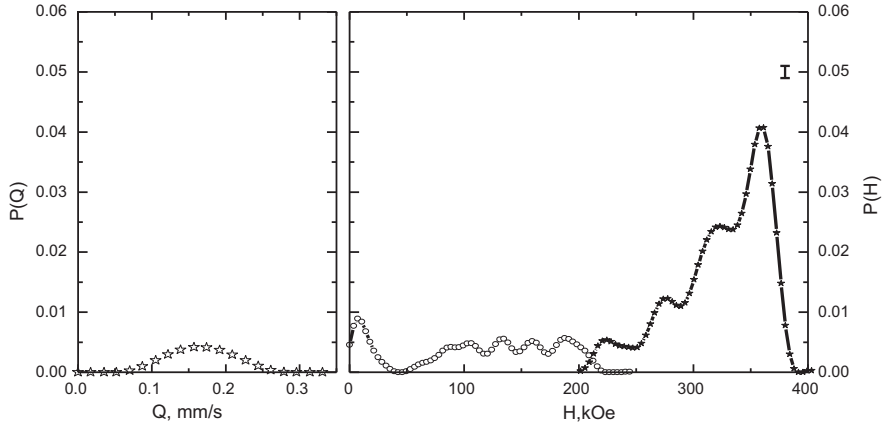

Fig. 6. Three-core distribution of the probability densities $P(H)$ and $P(Q)$ for the sample Fe–22Cr–15Co–9W annealed after quenching from 1150 °C and cold rolling.

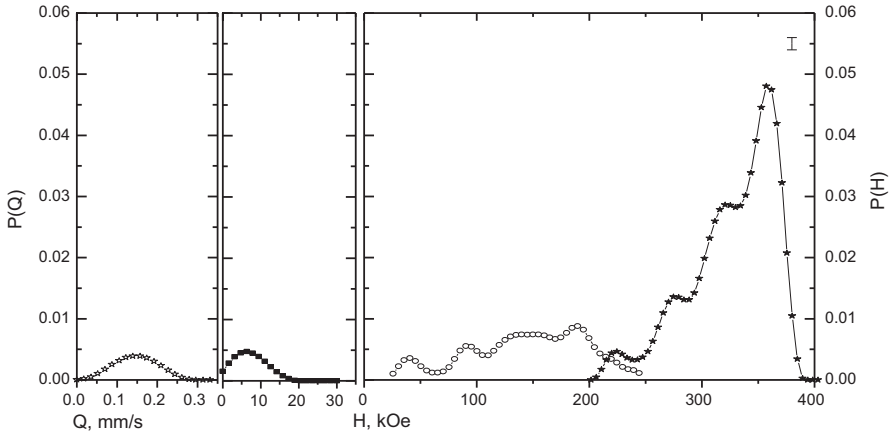

Fig. 7. Probability densities distributions $P(Q)$ and $P(H)$ for paramagnetic and magnetic spectral contributions taken in the model of four-core distribution for the alloy Fe–22Cr–15Co–9W annealed after quenching from 1150 °C and cold rolling.

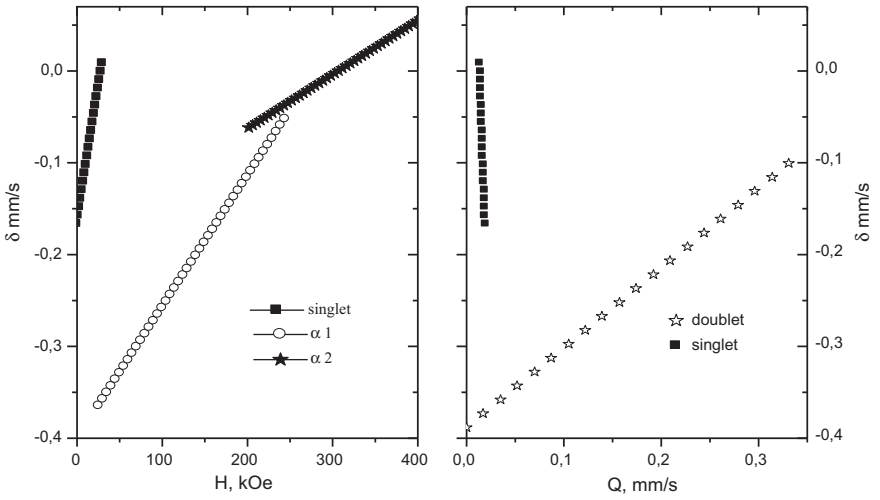

Fig. 8. Linear correlations of the parameters of the four-core distribution for the alloy Fe–22Cr–15Co–9W after annealed after quenching from 1150 °C and cold rolling (H is the hyperfine field; Q is the quadrupole splitting; δ is isomeric shift).

values and negative isomeric shifts, which means that η′ phase is enriched in tungsten and possibly chromium. This in turn points to the existence of a pronounced inhomogeneity in composition over the phase. Addition of Ga into the alloy does not affect in principal the form of both the Mossbauer spectrum and $P(H)$ and $P(Q)$ distributions and correlation dependences.

From the intensity of the paramagnetic doublet the fraction of iron involved into the η′ phase was estimated; in the alloys with different Ga content it amounts to (3–5)%. From the correlation dependences (Fig. 8) it follows that not all tungsten atoms are localized in the η′ phase; rather they are contained in the α_2 phase and regions responsible for the singlet as well. Suppose that 80% W atoms numbers in the η′ phase. In case the only other element in this phase is iron, its composition is estimated as close to equiatomic FeW. Taking into account the volumes of the unit cells of the α and η′ phases and the fact that each unit cell has 2 atoms, we yield the volume fraction of the η′ phase to be (5–6)%. This is somewhat lower than the volume fraction estimated from the electron microscopy data. Hence, it can be assumed that the η′ phase contains, along with iron and tungsten, chromium atoms as well.

It is not clear what the regions are represented by the singlet. Possibly, they are localized at the boundaries between the α_2 and η′ phases. In this case, these regions serve to transmit atoms between the α_2 and η′ phases and, consequently, all of them contain W.

4. Conclusions

Thus, the W enriched phase in the alloys Fe–Co–Cr–W–Ga is a metastable one, similarly to the η′ phase discovered by the authors of [6]. It has a body-centered tetragonal crystal lattice with the parameters $a \approx 2.96$ Å, $c \approx 3.17$ Å. After thermomechanical treatments resulting in the optimal combination of mechanical and magnetic properties in the alloys, the η′ phase has the form of disperse precipitates (40–70)–nm in size distributed over the matrix consisting of a mixture of strong magnetic (enriched in Fe–Co) and weak magnetic (enriched in Cr) phases. Between the lattices of the phase and matrix there are the orientation relationships under which $(\bar{1}\,\bar{1}\,0)$-α || $(1\,\bar{1}\,0)$-η′, $(\bar{3}\,1\,1)$-α || $(0\,\bar{1}\,1)$-η′, $(1\,\bar{3}\,1)$-α || $(1\,0\,\bar{1})$-η′ and $[1\,1\,2]$-α || $[1\,1\,1]$-η′.

The results obtained indicate that the phase contains, along with iron and tungsten, chromium and possibly cobalt and is quite inhomogeneous in composition. Feasibly, it is of variable composition. At room temperature the phase is paramagnetic.

Acknowledgements

The authors are grateful to Dr. M. Uimin for the fruitful discussion of the results.

The work was supported by the RFBR, project No. 11-02-91053-CNRS_a.

The electron microscopy studies were carried out in the Center of Electron Microscopy, and diffraction measurements, in the Department of X ray investigations of the Center of Collective Use, IMP, URAN, RAS.

References

[1] G.V. Ivanova, N.N. Shchegoleva, V.V. Serikov, N.M. Kleinerman, E.V. Belozerov, M.A. Uimin, V.S. Gaviko, N.V. Mushnikov, Phys. Met. Metallogr. 109 (5) (2010) 438–446.
[2] A.A. Novakova, T.Yu. Kiseleva, V.V. Lyovina, D.V. Kuznetsov, A.D. Dzidzigury, J. Alloys Compd. 317–318 (2001) 423–427.
[3] P.L. Grusin, Yu.L. Rodionov, Yu.A. Lu, Fiz. Met. Metalloved. 40 (1975) 1046–1052.
[4] T.B. Massalsky (Ed.), Binary Alloys Phase Diagrams, second ed., ASM International, 2001.
[5] Ya. Nemets, Structure and properties of intermetallic phases formed by transition metals, in: B. Stalinskii (Ed.), Physics and Chemistry of Solids, Chemistry Press, Moscow, 1972, pp. 7–41 (in Russian).
[6] E. Hornbogen, Zeit. Metallkde 52 (1) (1961) 47–56 (in German).
[7] V.S. Rusakov, Mossbauer Spectroscopy of Locally Inhomogeneous Systems, Alma-Ata, 2000 (in Russian).
[8] S. Alleg, B. Bouzabata, J.M. Greneche, J. Alloys Compd. 312 (2000) 265–272.